Global Change Biology

Global Change Biology (2010) **16**, 2062–2075, doi: 10.1111/j.1365-2486.2009.02064.x

# Net biome production of the Amazon Basin in the 21st century

BENJAMIN POULTER*,†, LUIZ ARAGÃO‡,§, URSULA HEYDER†, MARLIES GUMPENBERGER†, JENS HEINKE†, FANNY LANGERWISCH†, ANJA RAMMIG†, KIRSTEN THONICKE† and WOLFGANG CRAMER†

*Swiss Federal Research Institute for Forest, Snow, and Landscape Research (WSL), Zürcherstrasse 111, Birmensdorf 8903, Switzerland, †Potsdam Institute for Climate Impact Research (PIK), Telegraphenberg A26, D-14412 Potsdam, Germany, ‡School of Geography, University of Exeter, Exeter EX4 4RJ, UK, §Environmental Change Institute, Oxford University, Oxford OX1 3QY, UK

## Abstract

**Global change includes multiple stressors to natural ecosystems ranging from direct climate and land-use impacts to indirect degradation processes resulting from fire. Humid tropical forests are vulnerable to projected climate change and possible synergistic interactions with deforestation and fire, which may initiate a positive feedback to rising atmospheric $CO_2$. Here, we present results from a multifactorial impact analysis that combined an ensemble of climate change models with feedbacks from deforestation and accidental fires to quantify changes in Amazon Basin carbon cycling. Using the LPJmL Dynamic Global Vegetation Model, we modelled spatio-temporal changes in net biome production (NBP); the difference between carbon fluxes from fire, deforestation, soil respiration and net primary production. By 2050, deforestation and fire (with no $CO_2$ increase or climate change) resulted in carbon losses of 7.4–20.3 Pg C with the range of uncertainty depending on socio-economic storyline. During the same time period, interactions between climate and land use either compensated for carbon losses due to wetter climate and $CO_2$ fertilization or exacerbated carbon losses from drought-induced forest mortality (−20.1 to +4.3 Pg C). By the end of the 21st century, depending on climate projection and the rate of deforestation (including its interaction with fire), carbon stocks either increased (+12.6 Pg C) or decreased (−40.6 Pg C). The synergistic effect of deforestation and fire with climate change contributed up to 26–36 Pg C of the overall decrease in carbon stocks. Agreement between climate projections ($n = 9$), not accounting for deforestation and fire, in 2050 and 2098 was relatively low for the directional change in basin-wide NBP (19–37%) and aboveground live biomass (13–24%). The largest uncertainty resulted from climate projections, followed by implementation of ecosystem dynamics and deforestation. Our analysis partitions the drivers of tropical ecosystem change and is relevant for guiding mitigation and adaptation policy related to global change.**

*Keywords:* carbon cycle, climate change, deforestation, dynamic global vegetation model, fire, LPJmL

*Received 26 February 2009 and accepted 17 August 2009*

## Introduction

Global change encompasses multiple direct and indirect threats to ecosystems (Vitousek, 1994), the interactions of which present a challenge for impact assessment and implementing climate mitigation strategies. In tropical regions, ecosystem change is taking place rapidly due to the direct impacts of increasing deforestation (Houghton *et al*., 2000; Achard *et al*., 2002) and its indirect effects on forest integrity related to increasing fire from intentional and accidental ignitions (Cochrane *et al*., 1999; Morton *et al*., 2008). Tropical forest loss is also enhanced during drought years where the synergistic effects of deforestation, fire and climate cause widespread degradation or conversion of forest to nonforest habitat (Aragão *et al*., 2008; Barlow & Peres, 2008).

Tropical regions are vulnerable to climate change because changes in the seasonality and magnitude of precipitation can lead to large water deficits followed by increased forest mortality and decreased productivity (Clark *et al*., 2003; Nepstad *et al*., 2007). Earth system models have identified the Amazon Basin as vulnerable to ecosystem collapse or 'dieback' because of climate

Correspondence: Benjamin Poulter, Swiss Federal Research Institute for Forest, Snow, and Landscape Research (WSL), Zürcherstrasse 111, Birmensdorf 8903, Switzerland, e-mail: Benjamin.Poulter@wsl.ch

change induced drought and increasing air temperature leading to widespread forest mortality and the release of large amounts of carbon to the atmosphere (Cramer *et al*., 2004; Cox *et al*., 2004, 2008; Sitch *et al*., 2008). The interactions between deforestation, fire, and climate change in the Amazon Basin impact global biogeochemistry, biodiversity, and climate; however, the combined effects of these drivers remain poorly understood and the feedback-strength inadequately quantified (Soares-Filho *et al*., 2006; Malhi *et al*., 2008; Cochrane & Barber, 2009). Improving our understanding of spatio-temporal dynamics of tropical forest change is necessary to implement local, regional, and global climate mitigation policies as well as to reduce uncertainty on the effectiveness of forest adaptation and mitigation on climate change (Van Vuuren *et al*., 2008).

In the policy context, strategies for adapting tropical forests to climate change or to mitigate $CO_2$ emissions through carbon sequestration, by conservation or active forest management, rely on projections of ecosystem dynamics across various spatial and temporal scales (Fearnside, 2001; Killeen & Solorzano, 2008; Nepstad *et al*., 2008). These management scenarios are also implemented across various levels of governmental and nongovernmental agencies and based on threat analysis or the identification of biodiversity or other ecosystem service hotspots, for example (Fearnside, 2003; Agrawal *et al*., 2008). At global scales, policies associated with the United Nations Framework Convention on Climate Change (UNFCCC) are motivated primarily by the Kyoto Protocol and more recently, Reduced Emissions through Deforestation and Degradation (REDD) (Gullison *et al*., 2007). At regional to local scales, mitigation and adaptation are carried out through local conservation approaches (Killeen & Solorzano, 2008) and forest restoration practices that promote biodiversity (Chazdon, 2008). In most cases, the long-term success of these policies would be enhanced if planning were better integrated with process-based modelling and the identification of ecosystem services and their vulnerability to global change.

Our current understanding of the spatio-temporal pattern of broad-scale threats to Amazon Basin ecosystems is one of several limiting factors to prioritizing the implementation of such adaptation and mitigation policies (Malhi *et al*., 2008). Nepstad *et al*. (2008) present various scales of planning criteria, that span from local to global, to avoid the Amazon 'tipping point' (Lenton *et al*., 2008) and possible positive carbon cycle feedbacks following deforestation, fire, and climate change. Their approach relies on information that provides indices of ecosystem services and their robustness over long time scales. At present, this type of approach is problematic because most impact assessment research has focused on the individual components of global change or have used equilibrium vegetation models, rather than comprehensive assessments where interactions and possible nonlinear responses may emerge (Cardoso *et al*., 2003; Cramer *et al*., 2004; Soares-Filho *et al*., 2006; Salazar *et al*., 2007; Golding & Betts, 2008).

In this study, we quantify the synergistic impacts of climate change and forest degradation and their feedback on carbon cycling in the Amazon Basin in order to quantify carbon dynamics and to identify regions where the implementation of mitigation and adaptation policies may be vulnerable. Specifically, we carried out a set of multifactorial simulations using a Dynamic Global Vegetation Model (DGVM) that included fire, deforestation, and climate change drivers and their various storylines to simulate Amazonian ecosystem dynamics through the 21st century. These storylines include nine climate model projections from the IPCC Fourth Assessment Report (AR4), two land-use scenarios from the SimAmazonia land-use model (Soares-Filho *et al*., 2006), and two forest fire scenarios that include accidental ignitions related to deforestation. We focused on the change in spatio-temporal dynamics of carbon stocks and fluxes within the basin by calculating net biome productivity (NBP) (Schulze *et al*., 2000). NBP balances carbon emissions from fire, deforestation, agricultural harvest, and ecosystem respiration fluxes with net primary production and indicates the carbon source-sink strength and possible positive feedback flux to atmospheric $CO_2$ concentrations.

## Materials and methods

### *Study region*

We modelled ecosystem dynamics for the entire Amazon Basin, 5.9 million $km^2$, which is mostly contained within Brazil (69%) and affected by Brazilian land-management policies (Nepstad *et al*., 2008). We focused in particular on Amazonian rainforests and savannah vegetation where the annual temperature and precipitation average 24.0–26.2 °C and $\sim$ 2100–2900 mm $yr^{-1}$ from southwest to northwest Amazonia (Malhi & Wright, 2004). Since the early 20th century, >13% of Amazonia has been deforested or degraded (Soares-Filho *et al*., 2006), and ongoing deforestation and slash and burn practices associated with road building are responsible for the continued conversion of forest to mechanized agriculture (e.g. soybean and livestock production) (Nepstad *et al*., 2006). Climate change projections for this region are uncertain (Fig. 1), while the majority of general circulation models (GCM) consistently project increasing temperature, precipitation changes vary both in the direction of change and in

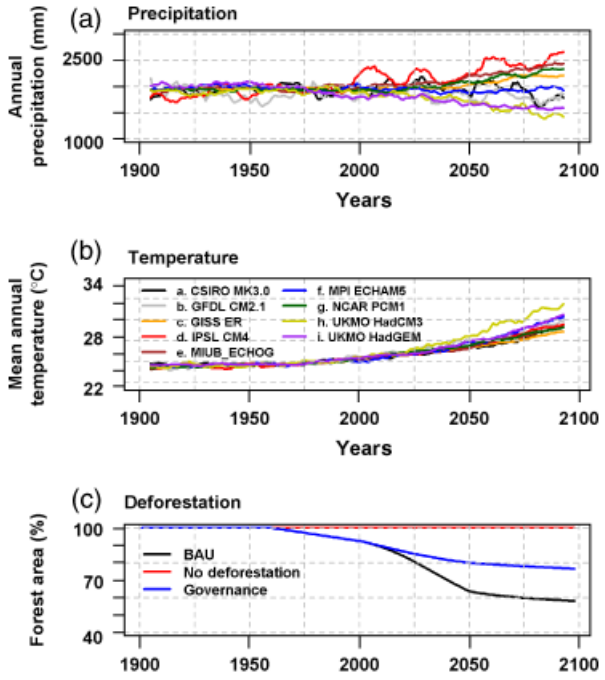


**Fig. 1** Mean annual climate projections, (a) precipitation (b) and temperature, for the entire Amazon Basin (smoothed with a 10-year moving average) used as inputs for LPJmL simulations. Nine GCMs were selected from the SRES A2 IPCC storyline. (c) deforestation trend for the entire Amazon Basin from Soares-Filho (2006) where BAU is business as usual.

the magnitude of change (Li *et al*., 2006; Malhi *et al*., 2009). The effects of climate change and elevated $CO_2$ may already be apparent in Amazonian ecosystems (Wright, 2005), indicated by increasing forest biomass (Baker *et al*., 2004), forest turnover (Phillips *et al*., 2004), and liana density (Phillips *et al*., 2002).

### *Simulation model*

We used the LPJmL DGVM (Sitch *et al*., 2003; Bondeau *et al*., 2007) to investigate transient Amazonian ecosystem responses to an ensemble of climate change scenarios, and a range of coupled forest fire and deforestation storylines. LPJmL includes natural, cropland, and pasture vegetation dynamics (Bondeau *et al*., 2007), natural fire disturbance (Thonicke *et al*., 2001), and improvements related to hydrologic processes (Gerten *et al*., 2004). Monthly air temperature, precipitation and cloud cover, described in 'Simulation protocol', are interpolated to quasi-daily values and used to simulate first-order physiological processes, such as photosynthesis and transpiration, which then determine vegetation composition and dynamics. Daily precipitation is distributed using a weather generator that randomly distributes daily rainfall volume over a known number of rain days in a month (Gerten *et al*., 2004). Soil type, which determines texture and water holding capacity, is determined from a global dataset (Zobler, 1986), and annual atmospheric $CO_2$ observations come from Carbon Dioxide Information Analysis Center (CDIAC) observations and projections from the Special Report on Emission Scenarios (Nakicenovic, 2000; Keeling & Whorf, 2005). The LPJ modelling framework has been evaluated at global and regional scales for boreal (Lucht *et al*., 2002), temperate (Zaehle *et al*., 2005), and tropical ecosystems (Cramer *et al*., 2004; Poulter *et al*., 2009) and the seasonal cycles of gross primary production (GPP) and carbon stocks are simulated within the range of tropical field observations (Poulter *et al*., 2009; Poulter *et al*., in review).

LPJmL simulates physiological processes, photosynthesis and transpiration on a daily time step using a Farquhar–Collatz canopy conductance scheme modified for global modelling purposes (Farquhar *et al*., 1980; Haxeltine & Prentice, 1996). Carbon allocation, vegetation dynamics for nine 'natural' plant functional types (PFT), fire disturbance, and land-use change are calculated annually. Individual, half-degree grid cells are partitioned to natural and managed land fractions composed of multiple potential crop types (Bondeau *et al*., 2007). Land-use fraction is input in a diagnostic mode (described in 'Land use dynamics') on an annual time step to determine specific crop fractions (Bondeau *et al*., 2007). The fire module, 'GlobFirm' has two main components, a burned area module and a vegetation mortality module (Thonicke *et al*., 2001). Burned area is empirically related to an annual fire season length index, which describes the probability of a fire occurrence. This index is calculated daily by relating simulated soil moisture to the 'moisture of extinction' (where fire can no longer spread) only when litter biomass is greater than a threshold of $200\,g\,m^{-2}$. PFTs are prescribed individual fire resistance parameters that determine the proportion of individuals that die each year (with mortality-related carbon returning to the atmosphere in the same year as a combustion flux). The existing fire model does not consider the role of human ignitions (which we update in 'Fire module updates'), generally resulting in underestimation of fire frequency where human use of fire is widespread (Thonicke *et al*., 2001).

### *Fire module updates*

In tropical Amazonia, fire frequency is strongly correlated with human land-use and deforestation (Cochrane *et al*., 1999; Nepstad *et al*., 1999; Cochrane, 2003; Morton *et al*., 2008). This is because few natural ignition sources exist and high fuel moisture typically stops or slows the spread of fire when an ignition does occur. Deforestation, however, increases the number of fire ignitions and

initiates a positive fire feedback cycle (Cochrane *et al*., 1999, Cochrane and Barber, 2009). This feedback cycle follows the first fire of an intact tropical forest, where tree mortality causes canopy openings and increased fuel loads. Subsequently, relative humidity drops and dead fuel accumulates, and dries faster, causing secondary ignitions to burn with higher intensity and severity. These wildfire dynamics are most common in frontier deforestation regions, whereas in more permanent agriculture areas, mechanized agriculture tends to reduce repeat fires (Morton *et al*., 2008).

To account for these feedbacks we added to the LPJmL Globfirm module a scalar related to the effect of human activities and land-use change on fire ignitions and fire season length. We parameterized the scalar using satellite remote sensing data of active fire counts, precipitation, and land use from the Brazilian Legal Amazon.

Active fire count (hot pixel) data were derived from a daily, 1 km spatial resolution, NOAA-12 database from the Brazilian Institute for Space Research (INPE) for the year 2000 (Aragão *et al*., 2007). Fire counts were aggregated to 0.25° resolution by summing the number of hot pixels over 1 year. Land cover data were acquired from the Vegetation Map of South America (Eva *et al*., 2002), which consists of 42 land cover classes at 1 km spatial resolution, classified from a multiresolution set of satellite data. We estimated agricultural cell fraction by summing the 1 km pixels classified as 'intensive agriculture' within each 0.25° spatial resolution cell and dividing by the total pixel area.

To parameterize the fire scalar, the annual fire count vector was normalized by the maximum number of counts so that the range was between 0 and 1. Agricultural cell fraction was then used as an independent variable to predict fire counts. The data followed a nonlinear function that was fitted with two parameters (Fig. 2). We estimated these parameters ($a$ and $b$) using a least-squares approach

$$F_s = a(\exp(-bA))A^2, \quad (1)$$

where $F_s$ is equal to the fire scalar, $a = 82.99 \pm 10.57$, $b = 6.77 \pm 0.32$, and $A$ is the grid cell agricultural fraction (0–1). The scalar, $F_s$, was then incorporated to GlobFirm to adjust the existing empirical relationship between fire season length and area burned using agriculture fraction input from the SimAmazonia dataset (see 'Land use dynamics').

Previous studies have shown that fire count data (i.e. hot pixels) are linearly related to area burned around the globe (Van der Werf *et al*., 2003; Giglio *et al*., 2006). This scalar, $F_s$, represents a combination of a theoretical, but data constrained, relationship between deforestation and the number of fire ignitions. Because of the spatial extent of the satellite data used in this analysis, the model is parameterized specifically for regional Amazon Basin simulations.

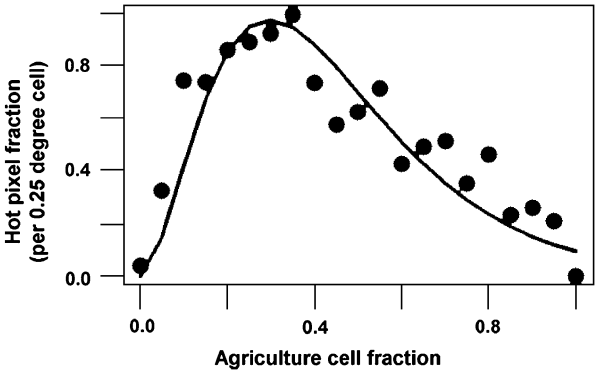


**Fig. 2** Relationship between agriculture cell fraction and fire count fraction from NOAA-12 satellite. As intact forest is deforested the pattern of agriculture is fragmented among many small plots. These small plots are more likely associated with accidental or intentional ignitions. More extensive agriculture is managed through mechanized farming, rather than fire, and repeat fires decrease. Solid line indicates the predicted fire effect from the model fit in Eq. (1).

### *Land use dynamics*

Land-use input data were prepared from the SimAmazonia dataset for a Business as Usual (BAU) and a Governance scenario (Soares-Filho *et al*., 2006). These data represent land cover at 1 km resolution for the years 2002–2050 for forest, nonforest, and deforested classes, using observational data from the Amazon Deforestation Monitoring Project (PRODES) as the 2002 baseline year (Soares-Filho *et al*., 2006). The SimAmazonia dataset models annual deforestation from statistically derived spatial relationships between forest cover, proposed road building, and regional socioeconomic projections (i.e. population growth).

To integrate the SimAmazonia land use simulations within LPJmL, the data were first aggregated to 0.5° resolution (matching the climate input data) and the 'deforested' category assigned to the grazing/pasture crop functional type (CFT) category, the most common form of land use following deforestation (Fearnside & Barbosa, 1998; Asner *et al*., 2004). To extend the dataset from 2002 back to 1901, required for the full transient model run, we assumed that rates of deforestation were minimal until 1960 because of evidence that intensive deforestation did not begin until the 1970s (Fearnside, 1996) and then used a simple linear interpolation to simulate forest loss until the 2002 land-use configuration was reached (similar to Houghton *et al*., 2000). The SimAmazonia land-use data were also extended to the year 2100 by extending the mean rate of deforestation

from 2046 to 2050 for each grid cell until either 80% of the grid cell had been deforested or until the protected area fraction of that grid cell was reached. We used the World Database on Protected Areas (WDPA) 2009 (Jenkins & Joppa, 2009) to estimate the grid cell fraction under protection. The $<80\%$ rule was implemented similar to previous modelling studies of tropical deforestation (Houghton *et al*., 2000; Cramer *et al*., 2004) and corresponds to a combination of more stringent future government land-use policies to slow deforestation and reduced access to forested areas because of a lack of road access.

The vegetation dynamics for the pasture cell fraction follow those described by Bondeau *et al*. (2007). Grasses are distinguished by two different photosynthetic pathways, $C_3$ and $C_4$, and their relative abundance is determined by climate and competition, with $C_4$ grasses predominant in tropical regions. Simulated disturbance (e.g. grazing by cattle) occurs when the grass leaf area index (LAI) reaches its maximum phenology and biomass, at this point, 50% of the aboveground biomass is consumed and released to the atmosphere, while 50% remains on site. Deforestation is determined on an annual time step, in this case, the current year natural cell fraction is compared with the new year managed land fraction. If the annual fraction of managed land is greater than the previous year, then the natural fraction is reduced (i.e. deforestation occurs). Selective logging is an important driver of forest structural change in the Amazon Basin (Asner *et al*., 2006). However, our simulated deforestation dynamics only represent even-age management (i.e. clearcutting) rather than selective logging because the forest stand dynamics in LPJmL follow a mean individual approach and age structure is not represented. The aboveground live biomass is harvest with 85% of sapwood and 100% heartwood and foliage removed as a carbon flux to the atmosphere, while 15% of sapwood enters the soil carbon pool directly (as fine and coarse roots).

### *Simulation protocol*

A complete set of factorial simulations were conducted with IPCC AR4 climate projection data (for the SRES A2 emissions scenario) and SimAmazonia land-use data (Soares-Filho *et al*., 2006). The SRES A2 emissions scenario was selected because recent observations show that atmospheric greenhouse gas concentrations most closely follow this trajectory and intensity of current greenhouse gas generation (Raupach *et al*., 2007). We selected nine GCM models (Fig. 1) based on a comparison of their performance against observed tropical Amazon Basin climate indices (Li *et al*., 2006, 2008; Malhi *et al*., 2009). These models have been shown to reproduce changes in the long-term trend of precipitation over the Amazon Basin (Li *et al*., 2008) and also represent a range of future climate projections for the region. The climate projection data were normalized to a common reference period (1961–1990) with data from the Climatic Research Unit (CRU) (New *et al*., 2002; Österle *et al*., 2003). An additional 'no climate change' scenario (including holding $CO_2$ concentrations at present levels) was generated to extend the CRU 1901–2007 climatology to the year 2100. This was accomplished by selecting annual climates from the 30-year time period 1978–2007 and randomly extending these from 2008 to 2100. A 1000-year model spin-up using the first 30 years of climate data (1901–1930) and preindustrial $CO_2$ concentrations was implemented to equilibrate soil carbon pools and vegetation dynamics. The transient climate simulations then began in 1901 and ended in 2098 (the common end year for the AR4 climate scenarios).

### *Data analysis*

We present results for changes from a baseline of 2003–2005 (the first years of the actual simAmazonia simulations based on observed land cover distribution) for vegetation, soil, and litter carbon stocks (Pg C), annual carbon fluxes (Pg C $yr^{-1}$), and tropical evergreen PFT cover (%). Annual NBP was calculated as

$$\mathrm{NBP} = (R + F + L + H) - (\mathrm{NPP} + E), \qquad (2)$$

where $R$ is ecosystem respiration, $F$ is fire carbon flux, $L$ is deforestation flux, $H$ is pasture harvest flux resulting from grazing, NPP is net primary production of the undisturbed forests, and $E$ is tree or grass seedling establishment flux on previously disturbed sites. Our calculation of NBP focuses only on terrestrial processes and we do not consider possible carbon export via river flow (Richey *et al*., 2002).

To summarize GCM projection uncertainty, we used methods similar to Scholze *et al*. (2006). For each GCM projection, we calculated the standard deviation ($\sigma$) of annual aboveground live biomass and NBP for the 2003–2005 time period. This was compared with the mean change for the 2045–2050 and the 2095–2098 time periods. An increase or decrease of the model variable of more than $\pm 1\sigma$ was considered ecologically significant. When applied to all GCM projections ($n = 9$), this approach allowed us to quantify the fraction of models in agreement with changes in NBP and aboveground live biomass.

## Results

### *Carbon stocks*

For the present climate, LPJmL simulated carbon stocks within the range of estimates from previous studies (see Fig. 3a for the complete range of above- and below-ground estimates) (Houghton *et al*., 2001; Saatchi *et al*., 2007). We estimated basin-wide aboveground live biomass as 80.53 Pg C with no land use and 74.8 Pg C with land use, within the range of Saatchi's *et al*. (2007) remotely sensed estimate for aboveground live biomass of 59–73 Pg C and the estimate of 39–93 Pg C for the Brazilian Amazon by Houghton *et al*. (2001), but lower than the estimate of Soares-Filho *et al*. (2006) of $119 \pm 23$ Pg C that assumed higher mean biomass per unit area than simulated here. The differences may also be attributed to the approach used by LPJmL to partition standing dead biomass directly into the litter and soil carbon pools, whereas bottom-up field based approaches frequently include both live and dead aboveground biomass in their estimates (Saatchi *et al*., 2007). Litter and soil carbon stocks were 7.2 and 34.5 Pg C, respectively, with no land use and 6.7 and 33.7 Pg C with land use, the difference reflecting increased litter inputs with higher aboveground live biomass. The simulated soil carbon estimates were also within the range of previous estimates of $36.4 \pm 3.4$ Pg C from bottom-up accounting approaches (Bernoux *et al*., 2002) and 28.3 Pg C of Milne *et al*. (2007). Total basin wide carbon (vegetation, soil, and litter carbon pools) was 109.5–122.2 Pg C, with and without land use.

Across climate and land-use storylines, there was large uncertainty in the transient dynamics of the aboveground carbon stocks (Fig. 4). By the year 2050, land-use change from deforestation reduced forest cover between 20% and 40% under the BAU and Governance land-use scenarios (and an additional 5–10% forest loss by 2100), respectively (Fig. 1c). The BAU deforestation scenario consistently reduced aboveground live biomass across all the climate projections; however, the loss of carbon under the lower rate of deforestation in the Governance scenario (Fig. 4), was compensated by wetter climate projections and $CO_2$ fertilization. In general, the changes in vegetation carbon stocks were more sensitive to the various storylines than the soil or litter pools, which had smaller standard error (Fig. 3b). The longer residence time of the soil carbon pool acted to buffer against interannual changes in climate, but quickly responded to changes in aboveground litter inputs with the soil carbon pool decreasing with deforestation.

For the entire basin, with no deforestation, projected decreases in aboveground biomass were consistent between models only 13–14% of the time in 2050 and 23–24% of the time in 2098 (Table 2a). Within the basin,

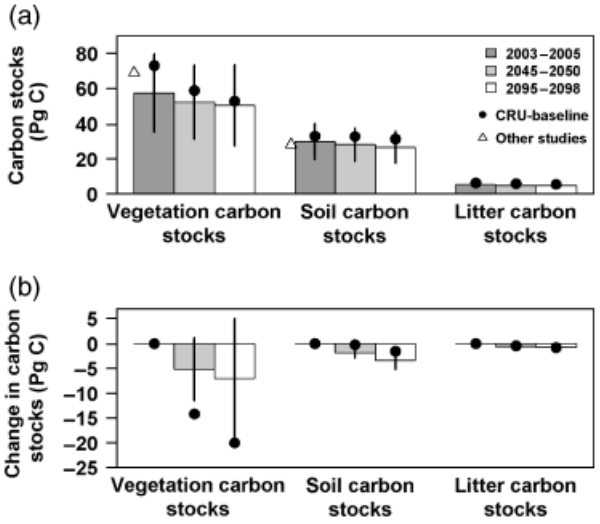


**Fig. 3** (a) Basin wide carbon stocks for three different time periods summarized for all climate and land-use storylines. (b) Changes in basin wide carbon stocks from 2003 to 2005 mean baseline summarized for all climate and land-use storylines. Error bars represent 1 SE summarizing the variability across all climate models. The CRU-baseline simulation is the result without climate change and reflects the 'equilibrium' ecosystem state.

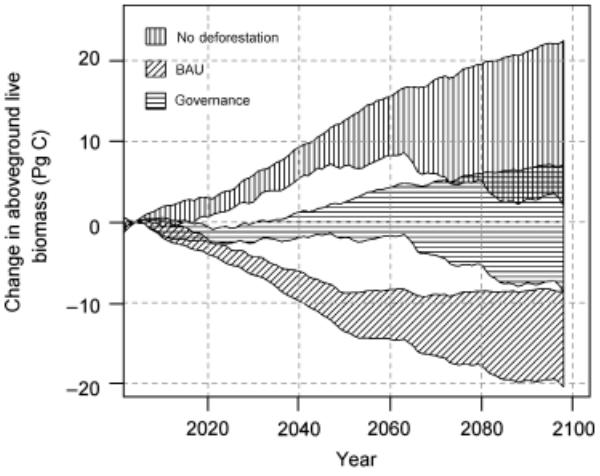


**Fig. 4** Change in basin-wide vegetation carbon relative to the 2003–2005 baseline. Envelope width represents 95% confidence interval for entire GCM ensemble.

most of the deforestation occurred within Eastern Amazonia, which was also where climate impacts on vegetation were characterized by higher agreement in the long-term climate projections (up to 75%). In Western Amazonia, there was much lower agreement regarding the direction and magnitude of aboveground biomass change among GCM models (Fig. 5), due to uncertainty in climate projections, with $<46\%$ of the GCMs in agreement over the long term (Table 2). The role of fire on vegetation carbon stocks had little effect on changes

in vegetation stocks for the moderate to wet scenarios, but became more important with its interaction with deforestation under drier climates (see 'Discussion').

### *Carbon fluxes*

For the baseline period, basin-wide NPP ranged between 5.6 and 5.7 Pg C $yr^{-1}$ (Fig. 6a) and was within the range of independent estimates from remote sensing and previous modelling approaches (Table 1). Basin-wide heterotrophic respiration was slightly higher under the no-deforestation scenario (5.2 Pg C $yr^{-1}$ compared with 4.8 Pg C $yr^{-1}$) because of the greater litter inputs from forest vegetation (Fig. 6a). Net ecosystem exchange (NEE) tended to be negative (a carbon sink) following all land-use storylines during the baseline period, and ranged from a flux of $-0.60$ Pg C $yr^{-1}$ with no deforestation to $-0.84$ Pg C $yr^{-1}$ with deforestation and fire, reflecting the lower soil respiration of the pasture ecosystems (where a negative flux represents a carbon sink).

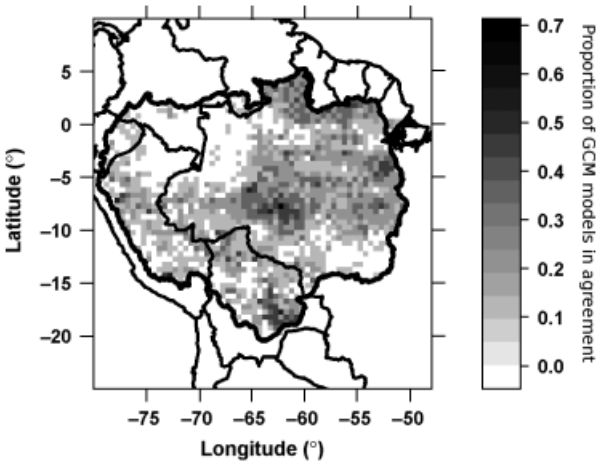


**Fig. 5** Proportion of GCMs in agreement with a decrease in aboveground live biomass of more than 1σ in 2095–2098 (compared with a 2003–2005 baseline) following Scholze *et al.* (2006).

The cumulative carbon fluxes from disturbance (fire, deforestation, and pasture grazing) were $\sim 0.73$ Pg C $yr^{-1}$ for the baseline period (Fig. 6a), compared with 0.1–0.4 Pg C $yr^{-1}$ from previous studies (Houghton *et al.*, 2000). The component fluxes were within the range of previous estimates (Table 1); simulated deforestation contributed between 0.18 and 0.22 Pg C $yr^{-1}$ (Fig. 3b) compared with 0.1–0.3 Pg C $yr^{-1}$ (Houghton *et al.*, 2000), fire emissions ranged between 0.20 and 0.29 Pg C $yr^{-1}$, and grazing/harvest emissions from pastures were 0.22 Pg C $yr^{-1}$. The interaction of deforestation with accidental fire ignitions resulted in an increase in the fire carbon flux by about 30% during the baseline period using the modified GlobFirm module (Fig. 6a).

Carbon fluxes, for all components, increased during the 21st century simulations (Fig. 6a and b). Up to 2050, NPP increased because of strong $CO_2$ fertilization and a relatively neutral climate effect (Fig. 1a and b). These

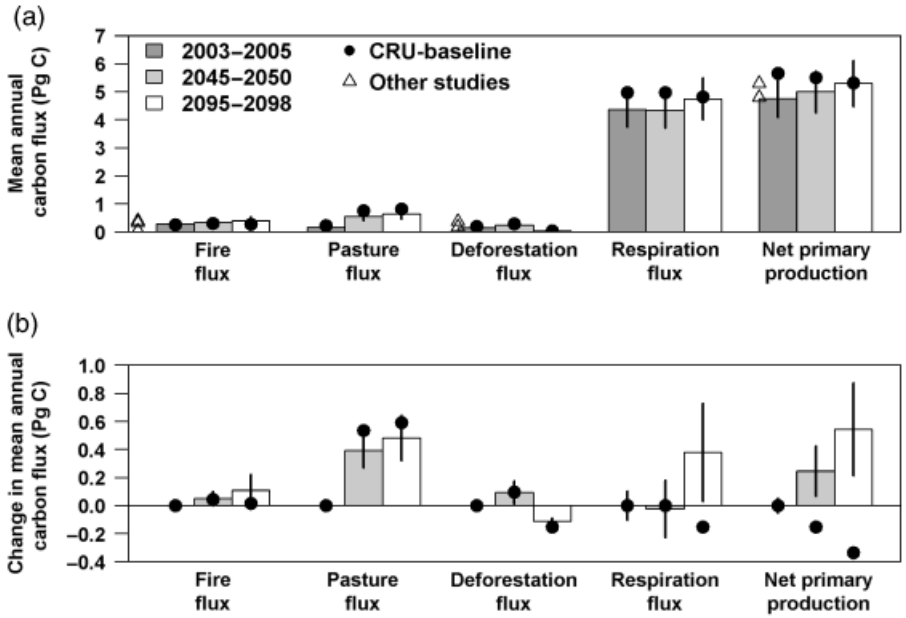


**Fig. 6** (a) Basin-wide carbon fluxes for three different time periods summarized for all climate and land-use storylines. (b) Changes in basin-wide carbon fluxes from 2003 to 2005 baseline summarized for all climate and land-use storylines. Error bars represent 1 SE summarizing the variability across all climate models. The CRU-baseline simulation is the result without climate change and reflects the 'equilibrium' ecosystem state.

**Table 1** Comparison of LPJmL fluxes with observations from modelling, remote sensing, and field studies

| Flux | LPJmL (2003–2005) ($Pg\,C\,yr^{-1}$) | Observation (including models, inversion, field studies) ($Pg\,C\,yr^{-1}$) | Extent | Reference |
|---|---|---|---|---|
| NPP | 5.6–5.7 | 4.8–5.9 (1980s)<br>3.8–5.9 | Brazilian Amazon | Potter *et al*. (2001), Tian *et al*. (1998) |
| NEE | −0.84 to −0.49 | −0.4 to 0.5<br>0.18<br>−3.0 to 0.75 | Amazonia | Potter *et al*. (2001), Houghton *et al*. (2000), Ometto *et al*. (2005) |
| Forest fire | 0.20–0.29 | 0.05 (1989–1998)<br>0.3–0.5<br>0.5<br>0.27–0.8<br>0.11–0.64 (future) | Brazilian Amazon<br>Central America/ northern South America<br>South America | Houghton *et al*. (2000), Cardoso *et al*. (2003), Van der Werf *et al*. (2003, 2004) |
| Deforestation flux | 0.17–0.22 | 0.18 (1989–1998)<br>0.35 (1970–1998)<br>0.30 (1996)<br>0.37 (0.19–0.53) (1980s) | Brazilian Amazon | Houghton *et al*. (2000), Hirsch *et al*. (2004), Nepstad *et al*. (1999), DeFries *et al*. (2002) |
| NBP (Eq. 2) | −0.49 to −0.15 | $0 \pm 0.2$ (1988–1998)<br>$-0.24\ (\pm 0.64)$ | Amazon/S. America | Houghton *et al*. (2000), Gurney *et al*. (2004) |

Not all flux variables were available for comparison, most notably, heterotrophic respiration. However, Basin wide net ecosystem exchange (NEE = *R*–NPP) and NPP are similar between observations and LPJmL simulations suggesting that heterotrophic respiration flux is reasonable.

climatic changes were accompanied by increasing rates of deforestation, fire, and pasture/grazing fluxes that influenced the overall trajectory of cumulative NBP. The total land-use carbon flux to the atmosphere due to deforestation (in the absence of fire, climate change, or $CO_2$ fertilization) ranged from 7.4 to 21.0 Pg C by 2050 (Table 3), slightly lower than Soares-Filho *et al*. (2006) estimate of aboveground vegetation losses of 15 to $32 \pm 8$ Pg C by 2050 (see 'Land use dynamics' for discussion). After the year 2060 (Fig. 4), increasing temperature acted to increase soil respiration and under some climate projections, decreasing precipitation had a negative effect on NPP and rates of mortality. Future carbon emissions from fire ranged from 0.25 to $0.51\,Pg\,C\,yr^{-1}$ in the year 2050 and $0.24–0.76\,Pg\,C\,yr^{-1}$ by 2098 with the range related to climate uncertainty and deforestation storylines (Fig. 3b).

*NBP*

LPJmL simulations for mean annual NBP were slightly negative, $-0.16$ to $-0.49\,Pg\,C\,yr^{-1}$ (i.e. a carbon sink), for all land-use and fire storylines during the baseline period (Table 1). The inclusion of land-use fluxes increased NBP (i.e. became less negative) because of the contribution of carbon losses to the atmosphere from deforestation, pasture grazing, and fire. There are a limited number of evaluation datasets for modelled NBP fluxes because by definition, it integrates over large temporal and spatial scales. Bottom-up accounting methods suggest that carbon fluxes from disturbance and productivity nearly balance one another in the Brazilian Amazon (Houghton *et al*., 2000) and top-down atmospheric inversion studies suggest a sink of $-0.24 \pm 0.64\,Pg\,C\,yr^{-1}$ or less (i.e. more positive) for South America (Gurney *et al*., 2004; Stephens *et al*., 2007) (Table 1).

Cumulative NBP reflected the synergistic effects of deforestation and climate change throughout the 21st century. The BAU deforestation storyline resulted in a cumulative carbon flux to the atmosphere of $\sim$ 14–28 Pg C, whereas the no deforestation scenario resulted in a continued strong regional carbon sink until $\sim$ 2060. Post 2060, respiration fluxes tended to increase due to higher temperature (Fig. 6b) and the storylines began to show a weakening of the regional carbon sink. Up to 2060, NBP carbon fluxes for the Governance scenario for deforestation were near zero, but became a carbon source following the combined effects of increasing temperature and decreasing precipitation in the mid–late 21st century.

Agreement among GCM models for increasing NBP was low (Table 2b). By 2050, 27–42% of the models agreed with an increase in NBP, which decreased in 2098, where 22–44% agreed. The spatial pattern of model agreement was highest in the first half of the 21st century while deforestation strongly determined carbon fluxes. By 2098, model agreement was lower because climate projections and their wide range of uncertainty was the main driver of carbon fluxes.

**Table 2** Agreement (%) among climate projections ($n = 9$) for (a) a decrease in aboveground live biomass and (b) an increase in NBP, a weakening of the carbon sink ($< \pm 1\sigma$ from the baseline period)

| | Projection time period | | | | | |
|---|---|---|---|---|---|---|
| | 2045–2050 | | | 2095–2098 | | |
| Scenario | East | West | Basin | East | West | Basin |
| *(a)* | | | | | | |
| *No fire* | | | | | | |
| Climate change | 17.7 | 8.2 | 13.5 | 30.7 | 15.3 | 23.9 |
| Climate change and deforestation (Governance) | 46.9 | 26.1 | 37.7 | 54.7 | 33.5 | 45.3 |
| Climate change and deforestation (BAU) | 72.1 | 34.3 | 55.4 | 77.5 | 44.1 | 62.8 |
| *Fire* | | | | | | |
| Climate change | 18.6 | 8.9 | 14.3 | 31.4 | 15.8 | 24.5 |
| Climate change and deforestation (Governance) | 53.4 | 30 | 43.1 | 57.4 | 36.3 | 48.1 |
| Climate change and deforestation (BAU) | 75 | 38 | 58.6 | 81 | 46.9 | 65.9 |
| *(b).* | | | | | | |
| *No fire* | | | | | | |
| Climate change | 22.2 | 19.9 | 21.2 | 35.1 | 38.1 | 36.4 |
| Climate change and deforestation (Governance) | 25.1 | 25.4 | 25.2 | 28.5 | 39 | 33.2 |
| Climate change and deforestation (BAU) | 44 | 37.8 | 41.3 | 28.7 | 42.1 | 34.6 |
| *Fire* | | | | | | |
| Climate change | 22 | 17.8 | 20.1 | 39.1 | 36.1 | 37.8 |
| Climate change and deforestation (Governance) | 24.1 | 23.5 | 23.8 | 28.9 | 35.9 | 32 |
| Climate change and deforestation (BAU) | 41.1 | 35.4 | 38.6 | 27.3 | 38.4 | 32.2 |

East and western regions of the Amazon Basin are defined by $-65.5^{\circ}$ longitude.

**Table 3** Mean change in total above and belowground carbon stocks (Pg C) from baseline period (2003–2005)

| Driver | 2045–2050 | 2095–2098 |
|---|---|---|
| *No fire, no deforestation* | | |
| No climate change | 3.3 | 0.6 |
| Climate change and $CO_2$ | 10.04 (3.2 to 16.1) | 14.06 (−16.6 to 33.1) |
| *Fire* | | |
| No climate change | 3.3 | 0.2 |
| Climate change and $CO_2$ | 9.22 (2.9 to 16.3) | 13.69 (−19.0 to 33.5) |
| *Deforestation* | | |
| No climate change | −13.75 (−20.1 to −7.4) | −22.15 (−30.5 to 13.8) |
| With climate change and $CO_2$ | −7.55 (−20.1 to 4.3) | −11.58 (−39 to 12.6) |
| *Fire + deforestation* | | |
| No climate change | −14.35 (−20.3 to −8.4) | −22.3 (−30.1 to −14.5) |
| With climate change and $CO_2$ | −8.49 (−19.9 to 3.2) | −12.67 (−40.6 to 12.1) |

Total carbon is sum of vegetation biomass, litter, and soil carbon pools. In parentheses are minimum and maximum simulated changes in carbon for the nine AR4 GCMs. The no climate change scenarios have no range because only the CRU climatology were used. Negative values represent a loss of carbon to the atmosphere.

## Discussion

### *Changes in Amazonian biogeochemistry*

Interannual variability in the Amazon Basin carbon cycle has a significant influence on global atmospheric chemistry (Rödenbeck *et al.*, 2003). During drought years, for example, anomalous increases in global atmospheric $CO_2$ come primarily from the Amazon Basin from a combination of fire, decreased productivity and increased ecosystem respiration (Rödenbeck *et al.*, 2003). Reducing uncertainty in future changes in the global carbon cycle depends on quantifying regional negative or positive feedbacks and their contribution to

rising atmospheric $CO_2$ concentrations, especially from tropical ecosystems (Cox *et al*., 2004; Sitch *et al*., 2008). Here, we show that the synergistic effects of climate, deforestation, and fire, are not simply 'additive' because of ecosystem feedbacks that exist to mitigate, or exacerbate, the exogenous drivers of stress. Process-based DGVMs provide an important perspective for understanding and partitioning these dynamics and their component fluxes. So far, previous accounting methods (Houghton *et al*., 2000; Soares-Filho *et al*., 2006) or equilibrium models (Salazar *et al*., 2007) have been unable to quantify the effect of these feedbacks and the magnitude of uncertainty. Because of the feedbacks identified by LPJmL and also because of the uncertainty among climate projections, changes in total carbon stocks have large ranges than previous acknowledged, and either increase by 33.5 Pg C or decrease by 40.6 Pg C due to climate, fire, and deforestation interactions by 2098 (Table 3). This range is somewhat smaller, and is more likely to be negative when only the deforestation scenarios are considered, with a decrease of 40.6–12.6 Pg C (Table 3).

Much of the modelled carbon cycle uncertainty is explained by ecosystem responses to GCMs that simulate either moderately wet future climates (GISS, IPSL, MIUB, and NCAR) or little change in precipitation and warming (CSIRO and GFDL). In contrast, the MPI and both the UKMO models project decreasing precipitation and warming temperatures resulting in reduced carbon stocks and NPP. We plotted the change in dry season length (number of months with $<100$ mm precipitation) with the change in aboveground live biomass for each of the deforestation and fire scenarios in Fig. 7. Aboveground live biomass decreases linearly with increasing dry season length, with the interaction between fire and deforestation more important with the more extreme drying scenarios. Climate evidently has the primary effect on the change in carbon stocks, with deforestation and fire having secondary effects. By contrast, we have also investigated ecosystem model parameter uncertainty and found it to be less important than climate model uncertainty for reducing our confidence in Amazonian carbon dynamics (B. Poulter, unpublished results).

The role of $CO_2$ fertilization was also important in our simulations, and caused an increase in photosynthetic rates and water-use efficiency as stomatal conductance decreases to maintain an optimal internal $CO_2$ concentration (following observations by Wong *et al*., 1979). Under the SRES A2 emissions scenario (used in this study) atmospheric $CO_2$ concentrations increase to about 850 ppm by the year 2100. This $CO_2$ fertilization effect has been shown to be significant in other continental-scale studies (Zaehle *et al*., 2007), where the authors showed NBP to become strongly negative in late 21st century Europe. Field experiments to evaluate tropical ecosystem responses to elevated $CO_2$ have yet to be conducted, but model sensitivity analyses have shown up to a 35% increase in tropical NPP (with no change in climate) at 550 ppm (Hickler *et al*., 2008), while here we show a $\sim 30\%$ change in NPP for our $CO_2$ and climate interaction scenarios. Such a strong tropical response to $CO_2$ may be realistic if water-use efficiency increases, but our simulations show that this response is not sustainable if precipitation declines beyond a certain level, which is also consistent with field and inversion studies that have shown tropical productivity is sensitive to drought (Clark *et al*., 2003; Rödenbeck *et al*., 2003).

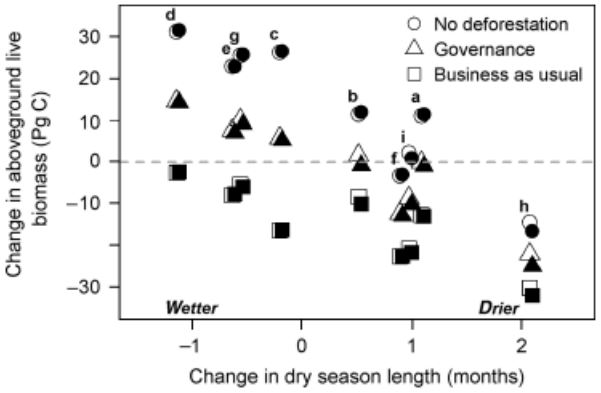


**Fig. 7** This figure illustrates the feedbacks modelled by LPJmL and shows the relationship between the change in dry season length (DSL) and the change in aboveground live biomass (Pg C) for each GCM and land-use/fire scenario. Filled (black) symbols are with fire, and the open (white) symbols are without fire. The letters above the points correspond to the climate models in Figure 1a and Figure 1b. The change in aboveground live biomass decreases linearly with increasing DSL and the interaction with fire and deforestation becomes more important with drying climates.

### *Terrestrial processes and their uncertainty*

To reduce the uncertainty of the Amazon Basin NBP dynamics, it is clearly necessary to reduce GCM uncertainty but also to reduce uncertainty of the socio-economic, land-use storylines and their implementation within the LPJmL framework. The disturbance flux components of NBP (i.e. deforestation, fire, and pasture grazing) may be more challenging to quantify compared with carbon fluxes derived directly from eco-physiological processes (i.e. photosynthesis and respiration). This is because of a larger uncertainty for scaling disturbance processes from heterogeneous field studies to ecosystem model formulations and their parameters (Ramankutty *et al*., 2007).

Our estimates for deforestation and fire fluxes are low in comparison with previous studies (Table 1). This is partly because the dynamics of residual carbon from deforestation are unclear, with some studies assuming all vegetation carbon is removed (Morton *et al.*, 2006) and other studies assuming a constant fraction remains (Soares-Filho *et al.*, 2006; Ramankutty *et al.*, 2007). Our fire carbon flux may also be low because it does not include fluxes from pasture fires, which can be significant sources of carbon fluxes (Guild *et al.*, 2004). However, in LPJmL litter biomass did not limit fire ignitions and was frequently above the $200\,g\,m^{-2}$ threshold, whereas high litter moisture reduced the probability of fire spread in simulated natural vegetation fraction. Partitioning the pasture harvest flux, which in 2050 reaches 0.54 and $0.97\,Pg\,C\,yr^{-1}$ under the Governance and BAU scenarios, to fire fluxes would also improve and increase our basin-wide fire carbon emissions. The high pasture flux is difficult to confirm because pasture management has not been scaled to the basin from field studies, but our $m^{-2}$ estimates of NPP are within the range of previous work $0.78\,kg\,C\,m^{-2}\,yr^{-1}$ compared with $0.9\,kg\,C\,m^{-2}\,yr^{-1}$ (Potter *et al.*, 1998).

### *Ecosystem feedbacks*

The feedbacks between climate, fire, and deforestation on tropical forest integrity have been recognized for some time, but only recently investigated in biogeochemical ecosystem models for tropical ecosystems (Nepstad *et al.*, 1999; Golding & Betts, 2008). Incorporating the effects of fire into earth system models (coupled climate, ocean, and ecosystem models) is considered one of the remaining challenges for the earth science community (Bowman *et al.*, 2009). While the LPJmL model does not include biophysical or biogeochemical feedbacks from fire and deforestation on climate, we illustrate that these interactions will have a large climate effect as they may add an additional $26\,Pg\,C$ to the atmosphere by 2098 (comparing the 'no fire, no deforestation and climate change' row with the 'fire, deforestation and climate change' row in Table 3). At the single grid cell scale (Fig. 8), the modelled interactions clearly show the synergistic effects; increasing temperature and decreasing precipitation cause an increase in fire emissions and decrease in aboveground carbon. The addition of deforestation activities cause fire emissions to increase further, combining with climate to increase carbon emissions. In comparison with previous studies, LPJmL uses similar root and soil depths to other models (Poulter *et al.*, 2009) suggesting that hydrologic responses should be similar, but the extent of Amazon dieback remains somewhat less severe (Cox *et al.*, 2004; Salazar *et al.*, 2007). LPJmL is somewhat less sensitive to temperature than other DGVM models (D. Galbraith, unpublished results) and the $CO_2$ feedback on water-use efficiency is ignored in equilibrium models (Salazar *et al.*, 2007).

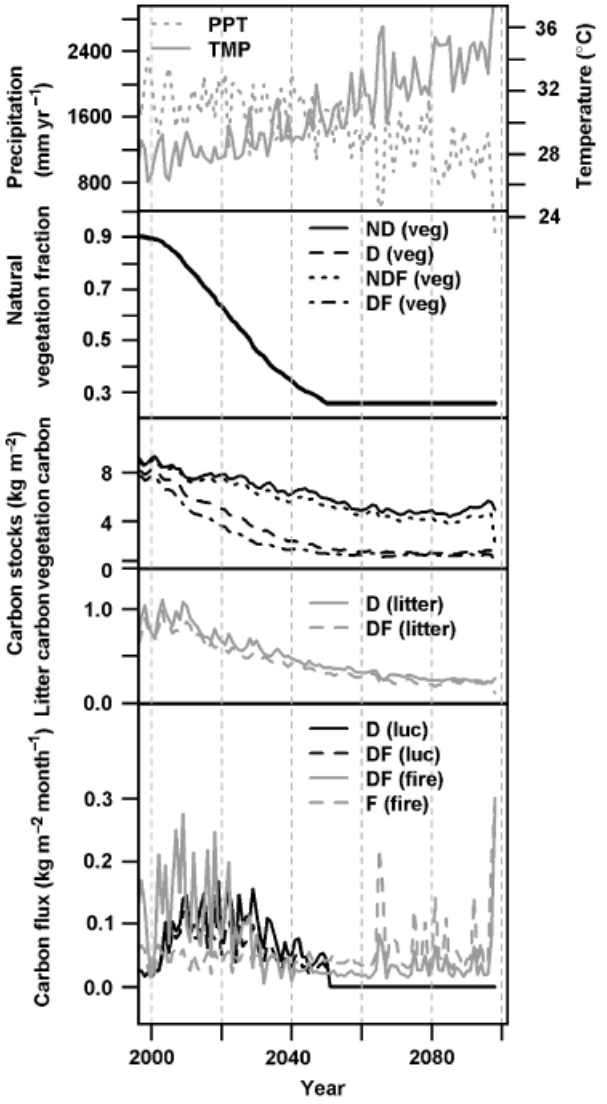


**Fig. 8** At the single grid cell level, climate–deforestation–fire interactions are clearly illustrated. As precipitation decreases and fuel loads dry, fire becomes more frequent causing carbon emissions to increase. Deforestation causes fire emissions to increase further due to accidental ignitions from encroaching road building and slash and burn agricultural practices. D, deforestation; ND, no-deforestation; F, fire.

### *Prioritizing mitigation and adaptation*

The spatio-temporal dynamics of GCM model agreement illustrates that uncertainty indices have the potential to inform adaptation and mitigation options

within the Amazon Basin. The large range of uncertainty from climate ensemble approaches makes it challenging for decision makers to anticipate impacts and policy responses (Cox & Stephenson, 2007). This study provides an example for estimating the range of ecosystem responses to climate and disturbance and can be used as informative weighting factors for prioritizing adaptation and mitigation strategies and to integrate process-based climate assessments with management planning (Scholze *et al*., 2006; Cox & Stephenson, 2007).

An application of this is illustrated by Nepstad *et al*. (2008), who recommend a hierarchical approach towards reducing the vulnerability of Amazonia to deforestation, fire, and land-use change. The hierarchy represents the different scales of governmental policies necessary to achieve a comprehensive sustainability strategy for Amazon ecosystems. At the local-scale, they recommend 'judicious use of fire' and a strategy that encourages alternative land-management practices and suppression. At local to regional scales, incentives to slow land-use transitions from forest to pasture combined with practices to improve pasture management. At regional scales, protected areas and minimizing road building efforts to slow associated deforestation are recommended. And finally, global policies, most notably associated with UNFCCC to provide incentives to reduce deforestation through REDD and ultimately mitigate climate change impacts. By isolating and identifying interactions between drivers on changes in Amazonian carbon stocks and fluxes, it will be possible evaluate and quantify the effectiveness of these various policies on avoiding the Amazon 'tipping point'.

## Conclusion

We present a modelling approach that quantifies the synergistic effects of the main drivers responsible for Amazon-related degradation responsible for 'tipping point' scenarios (Lenton *et al*., 2008; Nepstad *et al*., 2008). The multiple threats and limited resources to confront these threats requires that policies are implemented strategically both in space and time, as well as include the capacity to adapt to new threats as they emerge. These policies also take place within multiple sources of uncertainty that range from storylines to model variability (Cox and Stephenson 2007). Our results support previous findings that highlight direct land-use impacts as the predominant driver of ecosystem change in the short-term that are gradually overwhelmed by climate impacts and synergistic interactions in the long term.

## Acknowledgements

We appreciate funding from the Marie Curie FP6 Research Training Network 'Greencycles' (MRTN-CT-2004-512464). We thank the Natural Environment Research Council – UK for providing funds to Luiz Aragão (NE/F015356/1). We acknowledge the modelling groups, the Program for Climate Model Diagnosis and Intercomparison (PCMDI) and the WCRP's Working Group on Coupled Modelling (WGCM) for their roles in making available the WCRP CMIP3 multimodel dataset. Support of this dataset is provided by the Office of Science, US Department of Energy. Several anonymous reviewers provided valuable feedback on the manuscript and the development and implementation of the socio-economic storylines.

## References

Achard F, Eva HD, Stibig HJ, Mayaux P, Gallego J, Richards T, Malingreau JP (2002) Determination of deforestation rates of the world's humid tropical forests. *Science*, **297**, 999–1002.

Agrawal A, Chhatre A, Harding R (2008) Changing governance of the world's forest. *Science*, **320**, 1460–1462.

Aragão L, Malhi Y, Barbier N, Lima E, Shimabukuro Y, Anderson L, Saatchi S (2008) Interactions between rainfall, deforestation and fires during recent years in the Brazilian Amazonia. *Philosophical Transactions of the Royal Society B*, **363**, 1779–1785.

Aragão LEOC, Malhi Y, Roman-Cuesta RM, Saatchi SS, Anderson LO, Shimabukuro YE (2007) Spatial patterns and fire response of recent Amazonian droughts. *Geophysical Research Letters*, **34**, L07701, doi: 07710.01029/02006GL028946.

Asner GP, Broadbent EN, Oliviera PJ, Keller M, Knapp DE, Silva JNM (2006) Condition and fate of logged forests in the Brazilian Amazon. *Proceedings of the National Academy of Science*, **103**, 12947–12950.

Asner GP, Townsend AR, Bustamante MMC, Nardoto GB, Olander LP (2004) Pasture degradation in the central Amazon: linking changes in carbon and nutrient cycling with remote sensing. *Global Change Biology*, **10**, 844–862.

Baker TR, Phillips OL, Malhi Y *et al*. (2004) Increasing biomass in Amazonian forest plots. *Philosophical Transactions of the Royal Society of London*, **359**, 353–365.

Barlow J, Peres CA (2008) Fire mediated dieback and compositional cascade in an Amazonian forests. *Philosophical Transactions of the Royal Society B*, **363**, 1787–1794.

Bernoux M, Carvalho MCS, Volkoff B, Cerri CC (2002) Brazil's soil carbon stocks. *Soil Science Society of America*, **66**, 888–896.

Bondeau A, Smith PC, Zaehle S *et al*. (2007) Modelling the role of agriculture for the 20th century global carbon balance. *Global Change Biology*, **13**, 679–706.

Bowman DMJS, Balch JK, Artaxo P *et al*. (2009) Fire in the earth system. *Science*, **324**, 481–484.

Cardoso ME, Hurtt GC, Moore B III, Nobre CA, Prins EM (2003) Projecting future fire activity in Amazonia. *Global Change Biology*, **9**, 656–669.

Chazdon RL (2008) Beyond deforestation: restoring forests and ecosystem services on degraded lands. *Science*, **320**, 1458–1460.

Clark DA, Piper SC, Keeling CD, Clark DB (2003) Tropical rain forest tree growth and atmospheric carbon dynamics linked to interannual temperature variation during 1984–2000. *Proceedings of the National Academy of Science*, **100**, 5852–5857.

Cochrane MA (2003) Fire science for rainforests. *Nature*, **421**, 913–919.

Cochrane MA, Alencar A, Schulze MD, Souza Jr. CM, Nepstad DC, Lefebvre P, Davidson EA (1999) Positive feedbacks in the fire dynamic of closed canopy tropical forests. *Science*, **284**, 1832–1835.

Cochrane MA, Barber CP (2009) Climate change, human land use and future fires in the Amazon. *Global Change Biology*, **15**, 601–612.

Cox PM, Betts RA, Collins M, Harris PP, Huntingford C, Jones CD (2004) Amazonian forest dieback under climate-carbon cycle projections for the 21st century. *Theoretical and Applied Climatology*, **78**, 137–156.

Cox PM, Harris PP, Huntingford C *et al*. (2008) Increasing risk of Amazonian drought due to decreasing aerosol pollution. *Nature*, **453**, 212–216.

Cox PM, Stephenson D (2007) A changing climate for prediction. *Science*, **317**, 207–208.

Cramer W, Bondeau A, Schaphoff S, Lucht W, Smith B, Sitch S (2004) Tropical forests and the global carbon cycle: impacts of atmospheric carbon dioxide, climate change and rate of deforestation. *Philosophical Transactions of the Royal Society of London*, **359**, 331–343.

DeFries R, Houghton RA, Hansen MC, Field CB, Skole DL, Townsend J (2002) Carbon emissions from tropical deforestation and regrowth based on satellite observations for the 1980s and the 1990s. *Proceedings of the National Academy of Science*, **99**, 14256–14261.

Eva HD, de Miranda EE, Di Bella CM *et al*. (2002) A vegetation map of South America. Joint Research Centre, Brussels, Belgium, EUR 20159 EN.

Farquhar GD, von Caemmerer S, Berry JA (1980) A biochemical model of photosynthetic $CO_2$ assimilation in leaves of $C_3$ plants. *Planta*, **149**, 78–90.

Fearnside PM (1996) Amazonian deforestation and global warming: carbon stocks in vegetation replacing Brazil's Amazon forest. *Forest Ecology and Management*, **80**, 21–34.

Fearnside PM (2001) The potential of Brazil's forest sector for mitigating global warming under the Kyoto Protocol. *Mitigation and Adaptation Strategies for Global Change*, **6**, 355–372.

Fearnside PM (2003) Conservation policy in Brazilian Amazonia: understanding the dilemmas. *World Development*, **31**, 757–779.

Fearnside PM, Barbosa RI (1998) Soil carbon changes from conversion of forest to pasture in Brazilian Amazonia. *Forest Ecology and Management*, **108**, 147–166.

Gerten D, Schaphoff S, Haberlandt U, Lucht W, Sitch S (2004) Terrestrial vegetation and water balance – hydrological evaluation of a dynamic global vegetation model. *Journal of Hydrology*, **286**, 249–270.

Giglio L, van der Werf GR, Randerson JT, Collatz GJ, Kasibhatla P (2006) Global estimation of burned area using MODIS active fire observations. *Atmospheric Chemistry and Physics*, **6**, 957–974.

Golding N, Betts R (2008) Fire risk in Amazonia due to climate change in the HadCM3 climate model: potential interactions with deforestation. *Global Biogeochemical Cycles*, **22**, GB4007, doi: 10.1029/2007GB003166.

Guild L, Kauffman JB, Cohen WB, Hlavka CA, Ward DE (2004) Modeling biomass burning emissions for Amazon forest and pastures in Rondonia, Brazil. *Ecological Applications*, **14**, S232–S246.

Gullison RE, Fruhmhoff PC, Canadell JG *et al*. (2007) Tropical forests and climate policy. *Science*, **316**, 985–986.

Gurney KR, Law RM, Denning AS *et al*. (2004) Transcom 3 inversion intercomparison: model mean results for the estimation of seasonal carbon sources and sinks. *Global Biogeochemical Cycles*, **18**, GB1010, doi: 10.1029/2003GB002111.

Haxeltine A, Prentice IC (1996) A general model for the light-use efficiency of primary production. *Functional Ecology*, **10**, 551–561.

Hickler T, Smith B, Prentice IC, Mjofors K, Miller P, Arneth A, Sykes MT (2008) $CO_2$ fertilization in temperate FACE experiments not representative of boreal and tropical forests. *Global Change Biology*, **14**, 1531–1542.

Hirsch AI, Little WS, Houghton RA, Scott NA, White JD (2004) The net carbon flux due to deforestation and forest re-growth in the Brazilian Amazon: analysis using a process-based model. *Global Change Biology*, **10**, 908–924.

Houghton RA, Lawrence KT, Hackler JL, Brown S (2001) The spatial distribution of forest biomass in the Brazilian Amazon: a comparison of estimates. *Global Change Biology*, **7**, 731–746.

Houghton RA, Skole DL, Nobre CA, Hackler JL, Lawrence KT, Chomentowski WH (2000) Annual fluxes of carbon from deforestation and regrowth in the Brazilian Amazon. *Nature*, **403**, 301–304.

Jenkins CN, Joppa LN (2009) Expansion of the global terrestrial protected area system. *Biological Conservation*, **142**, 2166–2174.

Keeling CD, Whorf T (2005) *Trends: A Compendium of Data on Global Change*. Carbon DIoxide Information Analysis Center, Oak Ridge National Laboratory, Oak Ridge, TN.

Killeen TJ, Solorzano LA (2008) Conservation strategies to mitigate impacts from climate change in Amazonia. *Philosophical Transactions of the Royal Society B*, **363**, 1881–1888.

Lenton TM, Held H, Kriegler E, Hall JW, Lucht W, Rahmstorf S, Schellnhuber HJ (2008) Tipping elements in the Earth's climate system. *Proceedings of the National Academy of Science*, **105**, 1786–1793.

Li W, Fu R, Dickinson RE (2006) Rainfall and its seasonality over the Amazon in the 21st century as assessed by the coupled models for the IPCC AR4. *Journal of Geophysical Research*, **111**, D0211, doi: 10.1029/2005JD006355.

Li W, Fu R, Negron Juarez RI, Fernandes K (2008) Observed change of the standardized precipitation index, its potential cause and implications to future climate change in the Amazon region. *Philosophical Transactions of the Royal Society of London*, **363**, 1767–1772.

Lucht W, Prentice IC, Myneni RB *et al*. (2002) Climatic control of the high-latitude vegetation greening trend and Pinatubo effect. *Science*, **296**, 1687–1689.

Malhi Y, Aragão LEOC, Galbraith D *et al*. (2009) Exploring the likelihood and mechanism of a climate-change-induced dieback of the Amazon rainforest. *Proceedings of the National Academy of Science*, doi: 10.1073/pnas.0804619106.

Malhi Y, Roberts JT, Betts RA, Killeen T, Li W, Nobre C (2008) Climate change, deforestation, and the fate of the Amazon. *Science*, **319**, 169–172.

Malhi Y, Wright J (2004) Spatial patterns and recent trends in the climate of tropical rainforest regions. *Philosophical Transactions of the Royal Society of London*, **359**, 311–329.

Milne E, Paustian K, Easter M *et al*. (2007) An increased understanding of soil organic carbon stocks and changes in non-temperate areas: national and global implications. *Agriculture, Ecosystems and Environment*, **122**, 125–136.

Morton DC, deFries R, Randerson JT, Giglio L, Schroeder W, Van der Werf GR (2008) Agricultural intensification increases deforestation fire activity in Amazonia. *Global Change Biology*, **14**, 1–14.

Morton DC, DeFries RS, Shimabukuro YE *et al*. (2006) Cropland expansion changes deforestation dynamics in the southern Brazilian Amazon. *Proceedings of the National Academy of Science*, **103**, doi: 10.1073/pnas.0606377103.

Nakicenovic N), (Ed.) (2000) *Special Report on Emission Scenarios. Intergovernmental Panel on Climate Change (IPCC)*. Geneva, Switzerland.

Nepstad D, Stickler CM, Almeida OT (2006) Globalization of the Amazon soy and beef industries: opportunities for conservation. *Conservation Biology*, **20**, 1595–1603.

Nepstad D, Stickler CM, Soares-Filho B (2008) Interactions among Amazon land use, forests, and climate: prospects for a near-term forest tipping point. *Philosophical Transactions of the Royal Society B*, **363**, 1737–1746.

Nepstad D, Tohver IM, Ray D, Moutinho P, Cardinot G (2007) Mortality of large trees and lianas following experimental drought in an Amazon forest. *Ecology*, **88**, 2259–2269.

Nepstad D, Verissimo A, Alencar A *et al*. (1999) Large-scale impoverishment of Amazonian forests by logging and fire. *Nature*, **398**, 505–508.

New M, Lister D, Hulme M, Makin I (2002) A high-resolution data set of surface climate over global land areas. *Climate Research*, **21**, 1–25.

Ometto JPHB, Nobre AD, Rocha HR, Artaxo P, Martinelli LA (2005) Amazonia and the modern carbon cycle: lessons learned. *Oecologia*, **143**, 483–500.

Österle H, Gerstengarbe FW, Werner PC (2003) Homogenisierung und Aktualisierung des Klimadatensatzes der Climate Research Unit der Universität of East Anglia, Norwich. *Terra Nostra*, **6**, 326–329.

Phillips OL, Baker TR, Arroyo L *et al*. (2004) Pattern and process in Amazon tree turnover. *Philosophical Transactions of the Royal Society of London*, **359**, 381–407.

Phillips OL, Martinez RV, Arroyo L *et al*. (2002) Increasing dominance of large lianas in Amazonian forests. *Nature*, **418**, 770–774.

Potter C, Klooster S, de Carvalho CR *et al*. (2001) Modeling seasonal and interannual variability in ecosystem carbon cycling for the Brazilian Amazon region. *Journal of Geophysical Research*, **106**, 10423–10446.

Potter CS, Davidson EA, Klooster S, Nepstad D, de Negreiros GH, Brooks V (1998) Regional application of an ecosystem production model for studies of biogeochemistry in Brazilian Amazonia. *Global Change Biology*, **4**, 315–333.

Poulter B, Heyder U, Cramer W (2009) Modelling the sensitivity of the seasonal cycle of GPP to dynamic LAI and soil depths in tropical rainforests. *Ecosystems*, **12**, 517–533.

Ramankutty N, Gibbs HK, Achard F, DeFries R, Foley JA, Houghton RA (2007) Challenges to estimating carbon emissions from tropical deforestation. *Global Change Biology*, **13**, 51–66.

Raupach MR, Marland G, Ciais P, Le Quere C, Canadell JG, Klepper G, Field CB (2007) Global and regional drivers of accelerating $CO_2$ emissions. *Proceedings of the National Academy of Science*, doi: 10.1073/pnas.0700609104.

Richey JE, Melack JM, Aufdenkampe AK, Ballester VM, Hess LL (2002) Outgassing from Amazonian rivers and wetlands as a large tropical source of atmospheric $CO_2$. *Nature*, **416**, 617–620.

Rödenbeck C, Houweling S, Gloor M, Heimann M (2003) $CO_2$ flux history 1982–2001 inferred from atmospheric data using a global inversion of atmospheric transport. *Atmospheric Chemistry and Physics*, **3**, 1919–1964.

Saatchi SS, Houghton RA, dos Santos Alvala RC, Soares JV, Yu Y (2007) Distribution of aboveground live biomass in the Amazon Basin. *Global Change Biology*, **13**, 816–837.

Salazar LF, Nobre CA, Oyama MD (2007) Climate change consequences on the biome distribution in tropical South America. *Geophysical Research Letters*, **34**, L09708, doi: 10.1029/2007GL029695.

Scholze M, Knorr W, Arnell NW, Prentice IC (2006) A climate-change risk analysis for world ecosystems. *Proceedings of the National Academy of Science*, **103**, 13116–13120.

Schulze ED, Wirth C, Heimann M (2000) Managing forests after Kyoto. *Science*, **289**, 2058–2059.

Sitch S, Huntingford C, Gedney N *et al*. (2008) Evaluation of the terrestrial carbon cycle, future plant geography and climate-carbon cycle feedbacks using five Dynamic Global Vegetation Models (DGVMs). *Global Change Biology*, **14**, 2015–2039.

Sitch S, Smith B, Prentice IC *et al*. (2003) Evaluation of ecosystem dynamics, plant geography and terrestrial carbon cycling in the LPJ dynamic global vegetation model. *Global Change Biology*, **9**, 161–185.

Soares-Filho BS, Nepstad DC, Curran LM *et al*. (2006) Modelling conservation in the Amazon basin. *Nature*, **440**, 520–523.

Stephens BB, Gurney KR, Tans PP *et al*. (2007) Weak northern and strong tropical land carbon uptake from vertical profiles of atmospheric $CO_2$. *Science*, **316**, 1732–1735.

Thonicke K, Venevsky S, Sitch S, Cramer W (2001) The role of fire disturbance for global vegetation dynamics: coupling fire into a dynamic global vegetation model. *Global Ecology and Biogeography*, **10**, 661–677.

Tian H, Melillo JM, Kicklighter DW, McGuire AD, Helfrich JVK III, Moore B III, Vörösmarty CJ (1998) Effects of interannual climate variability on carbon storage in Amazonian ecosystems. *Nature*, **396**, 664–667.

Van der Werf GR, Randerson JT, Collatz GJ, Giglio L (2003) Carbon emissions from fires in tropical and subtropical ecosystems. *Global Change Biology*, **9**, 547–562.

Van der Werf GR, Randerson JT, Collatz GJ *et al*. (2004) Continental-scale partitioning of fire emissions during the 1997–2001 El Nino/La Nina period. *Science*, **303**, 73–76.

Van Vuuren D, Meinshausen M, Plattner GK *et al*. (2008) Temperature increase of 21st century mitigation scenarios. *Proceedings of the National Academy of Science*, **105**, 15258–15262.

Vitousek PM (1994) Beyond global warming: ecology and global change. *Ecology*, **75**, 1861–1876.

Wong S, Cowan IF (1979) Stomatal conductance correlates with photosynthetic capacity. *Nature*, **282**, 424–426.

Wright JS (2005) Tropical forests in a changing environment. *Trends in Ecology and Evolution*, **20**, 553–560.

Zaehle S, Bondeau A, Carter TR *et al*. (2007) Projected changes in terrestrial carbon storage in Europe under climate and land-use change 1990–2100. *Ecosystems*, **10**, 380–401.

Zaehle S, Sitch S, Smith B, Hattermann F (2005) Effects of parameter uncertainty on the modeling of terrestrial biosphere dynamics. *Global Biogeochemical Cycles*, **19**, GB3020, doi: 3010.1029/2004GB002395.

Zobler L (1986) A world soil file for global climate modeling. *NASA Technical Memorandum*, 32 pp.